Journal of Applied Research in Water and Wastewater
E - ISSN: 2476-6283
Journal homepage: https://arww.razi.ac.ir

Optimization of the operating parameters and their effects on the degradation of Naphthol Blue Black by the Fenton process

Salah Meddah[1,2], Imene Djeghader[2,3], Mohamed El Hadi Samar[1,2], Fadhel Ismail*[,2,3]

[1]*Environment Engineering Laboratory, University Badji-Mokhtar of Annaba, Algeria.*
[2]*Department of Process Engineering, Faculty of Engineering Sciences, University Badji-Mokhtar of Annaba, Algeria.*
[3]*Organic Synthesis Laboratory, Modeling and Optimization of Processes, University Badji-Mokhtar of Annaba, Algeria.*

GRAPHICAL ABSTRACT

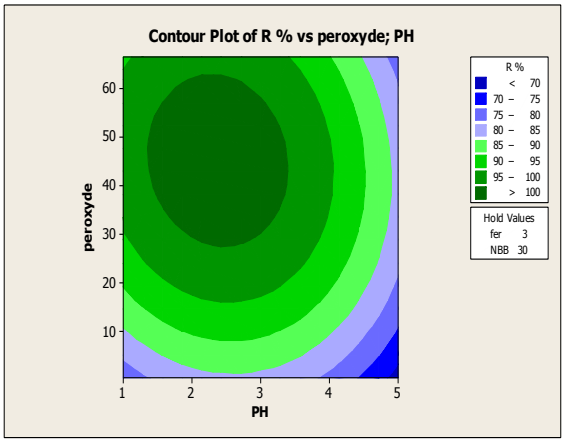

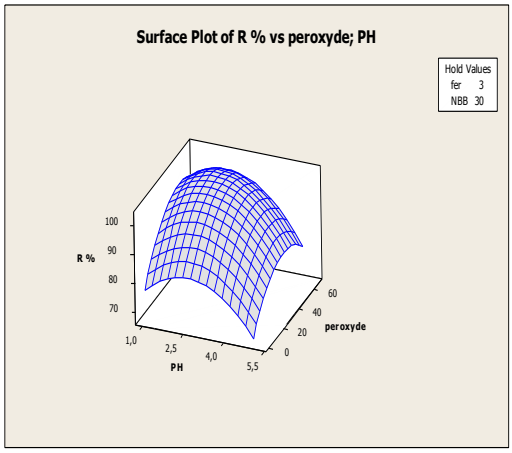

ARTICLE INFO

Article history:
Received 30 August 2021
Reviewed 9 November 2021
Received in revised form 4 December 2021
Accepted 6 December 2021
Available online 9 December 2021

Keywords:
Water treatment
Fenton process
Degradation
Azo dye
Experimental designs

Article type: Research Article

ABSTRACT

The objective of this work was to model and optimize the degradation of black azo dye Naphthol Blue Black (NBB) by the Fenton process (advanced oxidation) using a minimum of experiments. A Plackett-Burman screening design was first applied to determine the main factors influencing the process. The dye discoloration efficiency gave a yield approximately equal to 97 % in the best conditions of several operating parameters used. The variance analysis (ANOVA) showed the effects of all different factors and deduced the most important ones. Subsequently, a second quadratic design of experiments central composite type (CCD) was applied using the response surface methodology (RSM) to optimize the most important parameters deduced by the first design cited above, in order to obtain the best performance of the discoloration of NBB with this process. So from the contour plots and the response surfaces, the discoloration yield enhanced to the maximum and the optimization plot given by the Mnitab software, showed the following optimized parameters [NBB]=37.5 mg/L, [H_2O_2]=66.5 mg/L, [Iron]=3.5 mg/L and pH=3.4 for a yield of 100 % with a desirability of 1.0000. At last, to confirm that the discoloration was due to the degradation of the dye, the chemical oxygen demand (COD) was studied and in the optimized conditions, the degradation reached 94.78 % after 120 min of treatment. The kinetics of the dye degradation showed by the COD abatement was relatively slow compared to the kinetics of the dye discoloration.

1. Introduction

Most polluted effluents are very complex mixtures whose composition varies according to their industrial, agricultural or urban origin. Pollution assessment is therefore based on classifications according to the overall properties of the effluent. Pollution is defined as the introduction into a natural environment of foreign substances leading to its alteration. Harmful effects can occur at all levels (sanitary, ecological and economic) (Bouafia. 2010). Water pollution can be classified as flow pollution and stock pollution. The main difference between flow pollution and stock pollution is the persistence of environmental damage (Zhiyu. 2018). The textile industry consumes 80 % of all synthetic dyes applied to color 40x106 tons of textile products annually. After consumption, 15% of synthetic dyes are lost during manufacturing and processing. Due to their complex structures and synthetic origins, the effluents loaded with dyes are difficult to discolor; therefore, it becomes necessary to find alternative methods to treat pollutants that are recalcitrant to conventional treatments.

Azo dyes are the most preferred synthetic dyes for coating, leather dyeing, paper printing and textile dyeing because of their wide color spectrum, better firmness profile, simple application, inexpensive

*Corresponding author Email: ismail.fadhel@univ-annaba.org

Please cite this article as: S. Meddah, M.E.H. Samar, F. Ismail, Optimization of the operating parameters and their effects on the degradation of Naphthol Blue Black by the Fenton process, *Journal of Applied Research in Water and Wastewater*, 8 (2), 2021, 133-139.

synthesis, ease of structural modification, and ability to bind to most synthetic fibers (Wycliffe et al. 2019). In the modern textile industry, water management is particularly important. The amount of textile wastewater generated can reach more than 300 L per kg of product (Kallia and Talvenma. 2000).

The various conventional treatment technologies are unable to mineralize pollutants. Biological treatment technologies are also incapable for the degradation of pollutants because they are confined to easily biodegradable pollutants (Verma and Haritash. 2019). Advanced oxidation processes (AOPs) are the most efficient technologies for treating pollutants because they not only degrade pollutants but are also responsible for their efficient mineralization. Numerous studies carried out on a laboratory scale have clearly proven the efficiency of AOPs for the treatment of various effluents (Zaviska et al. 2009). Advanced oxidation processes (AOP) are booming. These are methods based on the formation of highly reactive chemical entities, this is the in situ formation of hydroxyl radicals $OH^{\bullet}$ which have a higher oxidizing power than traditional oxidants such as Cl_2, ClO_2 or O_3. These radicals are capable of partially or totally mineralizing most organic compounds (Verma and Haritash. 2019; Chergui–Bouafia and Alloune. 2007), the products are simple organic compounds, CO_2 and H_2O (Yingying Long et al. 2019; Ribeiro et al. 2017). Fenton-type reactions, in which Fe^{2+} ions are replaced by different species, have recently attracted more attention because they reduce costs and improve efficiency (Ribeiro et al. 2017).

Experimental designs are essentially a planning strategy to obtain sound and adequate conclusions in an efficient and cost-effective manner. The methodology of design of experiments is based on the fact that a properly organized experiment will often lead to simple analysis and statistics of the results (Iso 3534-3. 2013).

Experimental designs can be used in several scientific fields to study complex phenomena that require an enormous number of experiments to better understand how they work and optimize their performance (Benoist and Tourbier. 1994). This technique also allows us to obtain a maximum amount of information on the operating parameters and the influences of each of them as well as their interactions, which allows us to model them (Seong et al. 2003; Coupez and Nouatin. 1990). The objective of this work was to model and optimize the degradation of black azo dye blue Naphthol (NBB) by the Fenton process advanced oxidation using a minimum of experiments. A Plackett-Burman screening design was first applied to determine the most important parameters influencing the process. Subsequently, a second quadratic design of experiments central composite type (CCD) was applied using the response surface methodology (RSM) to optimize these parameters in order to obtain the best performance of the discoloration of NBB with this process. To confirm the degradation of the dye, the chemical oxygen demand (COD) and its kinetics were studied in the optimized conditions.

2. Material and methods

2.1. Chemicals

The different reagents used in this study were listed below were obtained as following: Zinc sulfate ($ZnSO_4.7H_2O$), sodium sulfate (Na_2SO_4) ferrous sulfate ($FeSO_4.7H_2O$) magnesium sulfate ($MgSO_4.7H_2O$) cobalt sulfate ($CoSO_4.7H_2O$), cadmium sulphate ($CdSO_4.8H_2O$) persulfate ($K_2S_2O_8$) perchloric acid ($HClO_4$), potassium chloride (KCl), tert butanol ($C_4H_{10}O_2$), propanol (C_3H_8O) and phenol C_6H_6O are supplied from Sigma-Aldrich. Hydrogen peroxide (H_2O_2) was purchased from Merck Com. Ammonium heptamolybdates tetrahydrate ($(NH_4)_6Mo7O_{24}.4H_2O$) and potassium iodide (KI) were obtained from Panreac and Riedel de Haen Com., respectively. Sulfuric acid (H_2SO_4), nitric acid (HNO_3), phosphoric acid (H_3PO_4), hydrochloric acid (HCl), sodium chloride (NaCl) and calcium chloride ($CaCl_2$) were obtained from Biochem Chemopharma Com.

2.2. Procedure

The oxidation of naphthol blue black by the fenton process was realized using an experimental device which comprises a perfectly stirred reactor (batch reactor) with a capacity of 1000 mL. The temperature of the bath (distilled water) was stabilized at the desired value by an immersion heater (tectron bio selecta thermostatted bath). The solution was continuously stirred by a mechanical agitator (Janke and KunKel RW 20). The agitator used was a propeller with four blades inclined at 45°. The pH of the solution being studied was measured using a pH electrode (Eutech Instruments). The temperature was controlled using a temperature sensor connected to the pH meter (Eutech Instruments). The oxidation of the dye was made in a discontinuous reactor with a volume of 1000 mL. The volume of the solution studied for all experiments was 500 mL. This volume was made up of: volume of the dye + volume of $FeSO_4$ + volume of H_2O_2 + volume of distilled water = 500 mL.

First, the dye solution was introduced in distilled water. Then, the acidify of the reaction medium was controlled with a few drops of concentrated acid to adjust the pH to the desired value (the volume of acid added is negligible). The temperature was set at the value chosen by the thermostat. The solution was mixed for a few minutes to homogenize the medium, then a known volume of $FeSO_4$ solution was introduced and at the end, the H_2O_2 solution was added to begin the reaction. In order to follow the oxidation kinetics, samples of 2 ml were taken at a specific time interval. The residual concentration of the dye in the solution at different times of sampling was determined by UV-visible spectroscopy. The concentration was determined from a calibration curve produced at pH 3 and a wavelength which corresponds to the maximum of absorbance (λ=619 nm), using a G705 Jenway spectrophotometer. The resolution of the wavelength and the bandwidth were 1nm and 0.5nm respectively, the cell was based on quartz and a thickness of 1cm. The rate of degradation or abatement of the color was calculated according to the Eq. 1.

$$Y_{col} = \left(1 - \frac{C_{tf}}{C_{t0}}\right) * 100 \quad (1)$$

where, C_{tf} and C_{to} correspond to the concentrations at final and at initial time, respectively.

3. Results and discussion

3.1. Effects of the operating parameters

3.1.1. Plackett-Burman design

The Plackett-Burman plan is very frequently used to study the effects of operating parameters. It is a double factor (i.e. −1 and +1) which identifies significant variables for the degradation of NBB by selecting "n" variables in the experiments. From the results previously found, nine parameters will be chosen in the present investigation, these parameters and their levels are presented in table 1. The experimental matrix and results according design of Plackett-Burman Design, are presented in Table 2. The main effect was calculated essentially as a difference between the measured mean of each variable performed at its high level (+1) and at its low level (−1). This design filtered variables based on a first-order model (Abdel-Fattah et al. 2002). This Plackett-Burman design is an essential tool for the selection of the effects of variables on performance of Fenton process. It can reduce significantly the number of repetitive experiments to be carried out.

3.1.2. Pareto diagram

From Minitab software, a graph of Pareto effects was used to identify the important factors (Fig. 1). The graph shows the main effect estimates plotted against the horizontal axis and includes a vertical line to indicate the threshold of statistical significance p = 0.05 (Bouziane et al. 2012). The Pareto diagram shows that the factors that have a major influence on the degradation of NBB are the pH (Kochany and Lipczynska-Kochany. 2009; Laiju et al. 2014; Alalm et al. 2014), the hydrogen peroxide [H_2O_2] concentration (Panda et al. 2011; Nidheesh and Rajan. 2016), the presence of chlorides (Tunçn *et al.* 2012; Grigorév et al. 1987), the nature of the acid used (Bouasla et al. 2010; Pignatello. 1992) and the temperature (Sun et al. 2007). The other parameters have less influence.

Table 1. Parameters and their intervals.

	C_0 NBB, mg/L	Fe^{2+}, mg/L	H_2O_2, mg/L	T, °C	$V_{agitation}$, rpm	pH	Acid	$CaCl_2$, g/L	$NaCl_2$, g/L
Min	10	1	1	20	100	1	H_3PO_4	0	0
Max	30	3	50	30	300	4	HNO_3	2	2

Table 2. Experimental results according Plackett-Burman design.

Run order	NBB, mg/L	T, ºC	$V_{agitation}$, rpm	Acid	$CaCL_2$, mg/L	NaCl, mg/L	Fe^{2+}, mg/L	pH	H_2O_2, mg/L	Yield, %
1	10	20	300	HNO_3	2	0	3	4	1	61.49
2	30	30	300	H_3PO_4	2	2	1	4	1	16.80
3	30	20	300	H_3PO_4	0	0	3	4	50	37.61
4	30	20	300	H_3PO_4	0	0	3	4	50	37.11
5	10	30	300	HNO_3	0	2	3	1	50	68.84
6	30	30	100	HNO_3	2	0	3	1	1	14.61
7	30	30	100	HNO_3	2	0	3	1	1	14.37
8	10	30	300	HNO_3	0	2	3	1	50	68.32
9	30	20	100	H_3PO_4	2	2	3	1	50	15.66
10	30	30	100	HNO_3	0	0	1	4	50	96.95
11	30	30	100	HNO_3	0	0	1	4	50	96.39
12	30	20	300	HNO_3	0	2	1	1	1	7.656
13	10	20	100	H_3PO_4	0	0	1	1	1	27.26
14	10	30	300	H_3PO_4	2	0	1	1	50	20.39
15	10	30	100	H_3PO_4	0	2	3	4	1	51.96
16	30	20	100	H_3PO_4	2	2	3	1	50	15.66
17	10	20	100	HNO_3	2	2	1	4	50	42.67
18	10	20	100	H_3PO_4	0	0	1	1	1	27.55
19	30	20	300	HNO_3	0	2	1	1	1	7.656
20	10	30	300	H_3PO_4	2	0	1	1	50	20.39
21	30	30	300	H_3PO_4	2	2	1	4	1	17.33
22	10	30	100	H_3PO_4	0	2	3	4	1	51.65
23	10	20	100	HNO_3	2	2	1	4	50	42.56
24	10	20	300	HNO_3	2	0	3	4	1	61.11

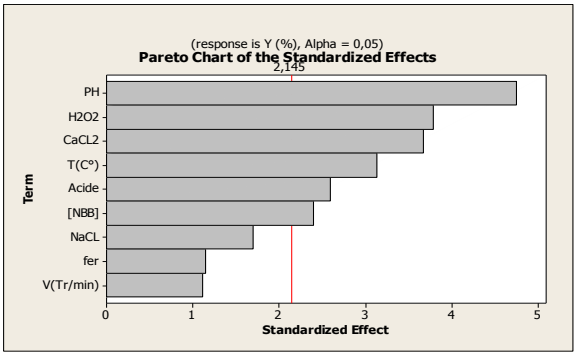

Fig. 1. Pareto diagram.

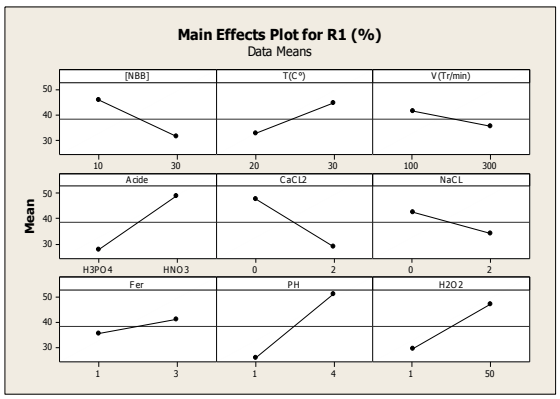

Fig. 2. Diagram of main effects.

3.1.3. Main effects

The main effects graph is most useful when we have several factors. The change in the average level can be compared to deduce the factors that most influence the response. For a factor with two levels, the response increases or decreases (positive or negative effect) from the lowest to the highest level, this difference is a “Main Effect” (Fig. 2). We talk about a significant effect if the probability is high (95.99 and 99.9 %) which means that the effect is "real" (Bouziane et al. 2012).

3.1.4. Analysis of variance

A variance analysis (ANOVA) is an essential tool for determining the meaning of an effect or a mathematical model. The most significant factors can be determined using a statistical parameter which is the P-value (Table 3). This P-value was compared to another Alpha value that represents the risk of the model. Generally, Alpha equals 5% of the risk. These results show that the effects of the pH (Kavitha and Palanivelu. 2005; Kwon et al. 1995; Nidheesh et al. 2013) of the solution as well as the acid used to fix it (Hammami et al. 2007; Gulkaya et al. 2006). The temperature (Ertugay and Acar. 2017), the presence of the salts (Arslan-Alaton et al. 2009), the concentration of the peroxide Xavier et al. 2015; Dulman et al. 2012) and that of the dye (Randrianantoandro et al. 2014; Lounis et al. 2016) are the most important and significant factors for NBB removal efficiency. The other factors are less important.

Table 3. Values of the variance analysis.

Term	Effect	Coefficient		Test of Fisher	P-value
		Coded	Uncoded		
Constant		38.545	6.2975	14.48	0
[NBB]	-14.417	-7.207	-0.72083	-2.71	0.017
T(C°)	12.022	6.011	1.20217	2.26	0.04
SS(Tr/min)	-6.138	-3.069	-0.0306	-1.15	0.268
Acid	21.255	10.627	10.627	3.99	0.001
$CaCL_2$	-18.875	-9.438	-9.437	-3.54	0.003
NaCl	-8.417	-4.208	-4.208	-1.58	0.136
Iron	5.828	2.914	2.914	1.09	0.292
pH	25.485	12.743	8.495	4.79	0
H_2O_2	17.925	8.962	0.3658	3.37	0.005

The Mathematical efficiency models as a function of coded and non-coded process parameters were determined with the regression coefficients in Table 3 (Eq. 2).

$$Y = A_0 + A_1X_1 + A_2X_2 + \ldots\ldots\ldots + A_nX_n \quad (2)$$

With, Y: the experimental response, X_n: coded (-1, +1) or non-coded variable, A_n: estimate of the main effect of factor "n" for Y response. According to our results represented in the previous Table 3, the modeling of the responses is written as follows:
-For coded units

$$Y = 38.545 - 7.207\ [NBB] + 6.011*T - 3.069*SS + 10.627*[acid] - 9.438*[CaCl_2] - 4.208*[NaCl] + 2.914*[Iron] + 12.743*pH + 8.962*[H_2O_2]$$

The dye discoloration efficiency gave a yield approximately equal to 97% in the best conditions of several operating parameters used (Table 2, Runs 10, 11).The variance analysis (ANOVA) showed the effects of all different factors and deduced the most important ones. These results are in accordance with previous study that gave for a temperature of 25±2 °C and pH=3, hydrogen peroxide concentration equal to 50 mg/, stirring speed equal to 250 rpm and an iron concentration of 3 mg/L, more than 98 % of the same dye [NBB] = 30 mg/L has been eliminated (Meddah et al. 2021).

3.2.2. Modeling of the degradation

Likewise for this method the analysis of variance is calculated in order to compare the relative significance of each parameter and to develop a polynomial model for the objective response which is the performance of the degradation of NBB in our study. The results found are introduced in the following Table 6. The model contains three linear effects, square and interaction effects. For the linearity which corresponds to the factors [iron], pH, $[H_2O_2]$ and [NBB], we note that the values of P are all greater than 0.05 except that for pH, so it can be seen that the latter has a significant effect on the yield of NBB degradation. The square effect is used to assess the existence of curvatures in the response surface. From the results in Table 5, it can be said that for the square effect only the pH and the concentration of hydrogen peroxide have a significant effect on the degradation performance of NBB. The variation in yield as a function of pH and the concentration of hydrogen peroxide will follow a curve instead of a straight line. For interactions, we note the existence of three effects which influence the yield of the degradation of NBB. These interactions are between: the concentration of hydrogen peroxide and pH, the concentration of iron and pH, the concentration of pollutant and pH. These interactions are shown in Figs. 3 and 4. From the different values of the coefficients determined for each operating parameter taken alone or combined (Table 5), we were able to write the equation of the yield model in its non coded unit:

$$Y = 88.6413 + 0.7457 * [H_2O_2] - 9.0275 * [iron] + 16.2624 * pH - 1.0096 * [NBB] - 0.0095 * [H_2O_2] * [H_2O_2] + 2.\ 2671 * [iron] * [iron] - 2.837 * pH * pH + 0.0165 * [NBB] * [NBB] - 0.0242 * [H_2O_2] * iron - 0.0294 * [H_2O_2] * pH + 0.\ 0084 * [H_2O_2] * [NBB] - 0.3938 * [iron] * pH - 0.0232 * [iron] * [NBB] - 0.0089 * pH * [NBB]$$

The last column of Table 4 presents the theoretical yield given by the model. Then, this makes it possible to calculate R^2 and adjusted R^2. Finally, since there are several insignificant terms, the values of R^2 and adjusted R^2 which are 53.47 % and 41.06 % respectively, seem to be just acceptable. If we remove the insignificant terms, the values of R^2 and adjusted R^2 will become too low. This is why the model must consider all of its terms.

3.2.3. Response surface methodology

In order to determine the operating conditions giving degradation yield greater than 90 %, we used the graphic method called the contour method. These contours or isoresponse surfaces are plotted as a function of two operating parameters. The surface diagram which is a three-dimensional graphical grid, represents the functional relationship between the response and the experimental factors. To draw these contours, we proceeded as follows: for each pair of operating parameters; for example $[H_2O_2]$ * pH, we have drawn three graphs. The first graph is plotted as a function of $[H_2O_2]$ * pH and the other parameters such as the concentration of the dye [NBB], the concentration of hydrogen peroxide $[H_2O_2]$. Their value is fixed at a level +1 or maximum value (Fig. 5).The second graph; the values of the other parameters are fixed at the mean level 0. The third graph the values of the other parameters are fixed at the minimum level or less than -1. Plotting the graphs in this way allows us to scan fairly broadly for each operating parameter. On the other hand, effects of iron and NBB are less important; indeed, the yield is between 95 and 100% in the intervals studied (Fig. 6).

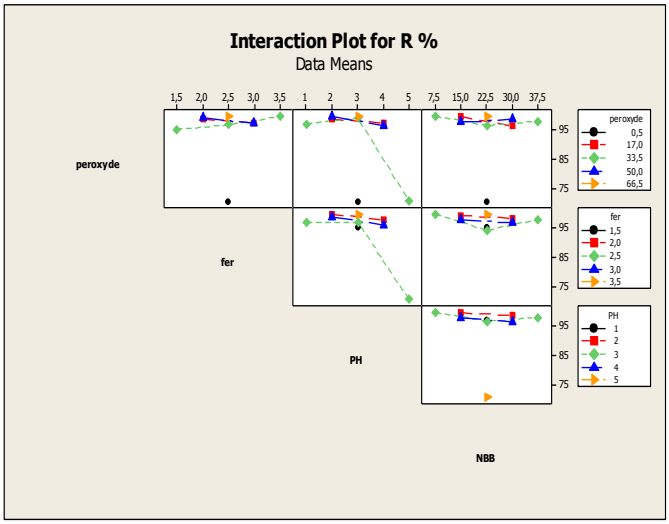

Fig. 4. Diagrams of interaction effects.

3.2.4. Optimization of the degradation parameters

The advantage of the optimization is to have a maximum yield for the degradation of NBB. From the four factors studied, we seek to find an optimal interval for which the yield will be at its maximum. For this, the optimization is applied under constraint. We choose different starting points in the dialog window area (optimized response) and a constraint on the targeted response. The results of the optimization indicate the optimal values for each factor as well as the optimal value of the degradation yield of the NBB. Fig. 7 shows an optimization under the following constraints; the target yield is 100.0 % with a desirability of 1.0000. Results for a degradation yield of 100 % are as following; for a $[NBB]_0$=37.5 mg/L, it is necessary that $[H_2O_2]$=66 mg / L, pH = 3.4 and [iron]=3.5 mg/L.

3.2.5. Chemical oxygen demand (COD)

The results represented in figure 8 clearly show that the use of the Fenton process with the optimum parameters for the degradation of NBB leads to a 94.78 % reduction in COD after 120 min of treatment. The kinetics of COD abatement is relatively slow compared to the kinetics of discoloration; this can be explained by the formation of intermediate products which require more time for them to be oxidized. Numerous studies have demonstrated the ability of the Fenton process to degrade a wide variety of azo dyes (Coupez and Nouatin. 1990; Lounis e al. 2016).

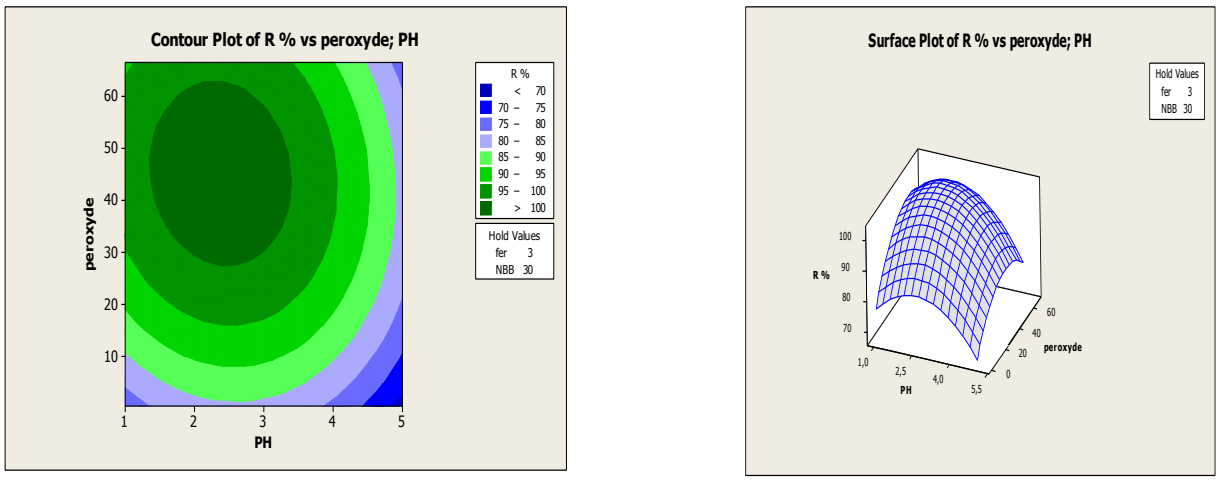

Fig. 5. Contour and response surface of the influence of pH and H_2O_2 on the yield.

Table 4. Matrix of experiences according to the central composite method.

Std Order	Run Order	Pt Type	Blocks	Peroxide, mg/L	Iron, mg/L	pH	NBB, mg/L	Experimental yield, %	Theoretical yield, %
25	1	0	1	33.5	2.5	3	22.5	100	99.94
21	2	-1	1	33.5	2.5	1	22.5	97.37	94.45
1	3	1	1	17	2	2	15	100	97.11
14	4	1	1	50	2	4	30	99.07	96.10
23	5	-1	1	33.5	2.5	3	7.5	100	104.71
5	6	1	1	17	2	4	15	100	92.75
19	7	-1	1	33.5	1.5	3	22.5	95.38	102.42
8	8	1	1	50	3	4	15	93.48	94.21
11	9	1	1	17	3	2	30	95.92	94.70
15	10	1	1	17	3	4	30	95.46	89.28
2	11	1	1	50	2	2	15	100	101.34
4	12	1	1	50	3	2	15	100	101.30
31	13	0	1	33.5	2.5	3	22.5	100	99.94
3	14	1	1	17	3	2	15	99.73	97.87
12	15	1	1	50	3	2	30	99.86	102.28
27	16	0	1	33.5	2.5	3	22.5	99.97	99.94
26	17	0	1	33.5	2.5	3	22.5	99.89	99.94
13	18	1	1	17	2	4	30	95.44	89.66
17	19	-1	1	0.5	2.5	3	22.5	70.26	84.66
16	20	1	1	50	3	4	30	96.51	94.93
7	21	1	1	17	3	4	15	99.94	92.73
30	22	0	1	33.5	2.5	3	22.5	100	99.94
10	23	1	1	50	2	2	30	99.92	102.67
9	24	1	1	17	2	2	30	99.86	94.29
28	25	0	1	33.5	2.5	3	22.5	100	99.94
22	26	-1	1	33.5	2.5	5	22.5	70.78	82.74
29	27	0	1	33.5	2.5	3	22.5	100	99.94
24	28	-1	1	33.5	2.5	3	37.5	98.27	102.60
18	29	-1	1	66.5	2.5	3	22.5	100	94.53
6	30	1	1	50	2	4	15	98.3	95.04
20	31	-1	1	33.5	3.5	3	22.5	100	102.00

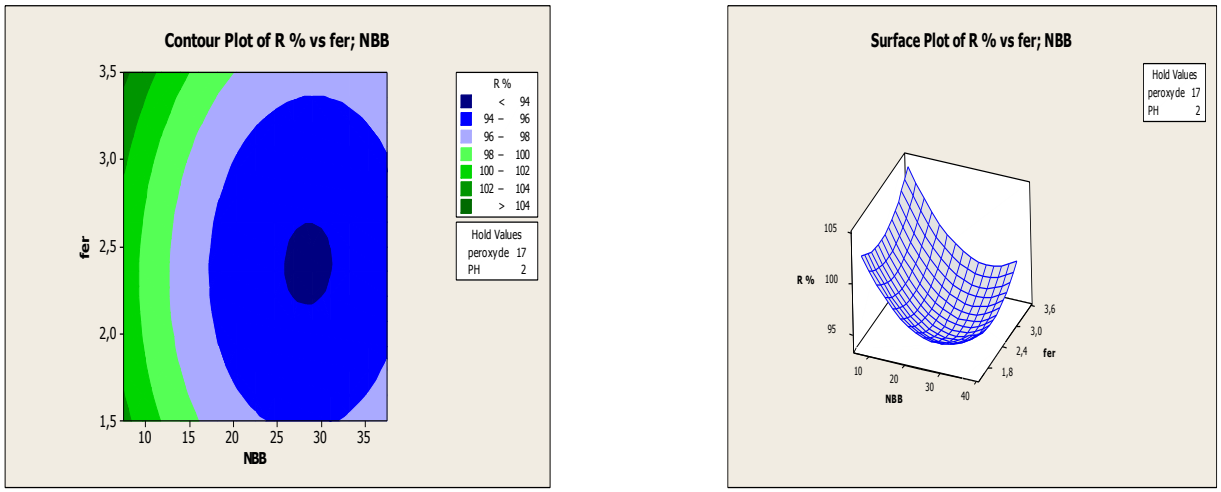

Fig. 6. Contour and response surface of the influence of iron and NBB on the yield.

Table 5. Analysis of variance for the composite design.

Term	Coefficient		Test of Fisher	P-value
	Coded	Uncoded		
Constant	88.6413	59.5689	1.488	0
Peroxide	0.7457	0.751	0.993	0.156
Iron	-9.0275	30.239	-0.299	0.589
pH	16.2624	13.08	1.243	0.053
NBB	-1.0096	1.744	-0.579	0.391
$(Peroxide)^2$	-0.0095	-0.0095	0.0047	0.024
Iron*Iron	2.2671	5.0981	0.445	0.346
pH*pH	-2.837	1.2745	-2.226	0.002
NBB*NBB	0.0165	0.0227	0.728	0.152
peroxide*Iron	-0.0242	0.2065	-0.117	0.091
peroxide*pH	-0.0294	0.1033	-0.284	0.008
peroxide*NBB	0.0084	0.0138	0.608	0.060
Iron*pH	-0.3938	-0.116	-0.116	0.031
Iron*NBB	-0.0232	-0.051	-0.051	0.230299
pH*NBB	-0.0089	-0.039	-0.039	0.0208012

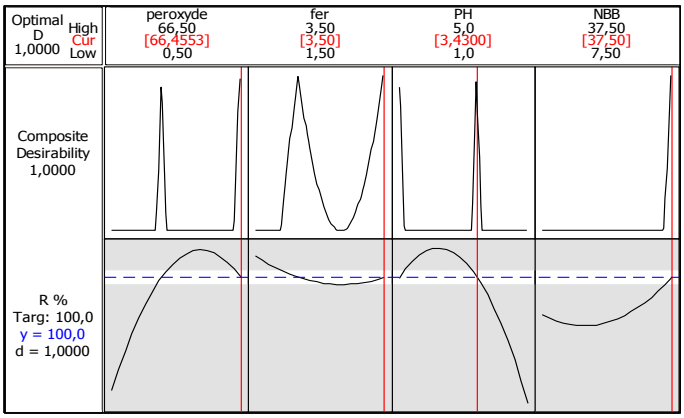

Fig. 7. Optimization plot.

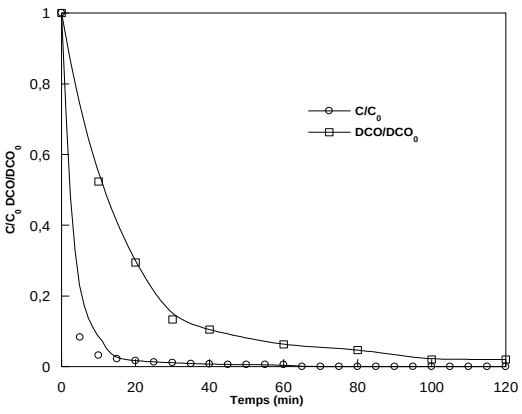

Fig. 8. Kinetics of the NBB degradation.

4. Conclusions

In this work we have studied the influence of operating parameters on the Fenton process advanced oxidation efficiency of a solution contaminated by an azo dye which is Naphthol Blue Black. A Plackett-Burman screening design was first applied to determine the main factors influencing the process. The dye discoloration efficiency gave a yield approximately equal to 97% in the best conditions of nine operating parameters used. The variance analysis showed the effects of all these different factors and were deduced the most important ones which will be optimized with a second-order experimental design. However; a second quadratic design of experiments central composite type was applied using the response surface methodology to optimize the parameters deduced by the first design cited above, in order to obtain the best performance of the discoloration of NBB with this process. So from the contour plots and the response surfaces, the discoloration yield enhanced to the maximum and the optimization plot given by the Mnitab software, showed the following optimized parameters [NBB]=37.5 mg/L, [H_2O_2]=66.5 mg/L, [Iron]=3.5 mg/L and pH=3.4 for a yield of 100% with a desirability of 1.0000. The discoloration was due to the degradation of the dye, indeed the chemical oxygen demand showed that the degradation reached 94.78% after 120 min of treatment. The kinetics of the dye degradation was relatively slow compared to the kinetics of the dye discoloration.

Nomenclature

ANOVA	Analysis of variance
AOPs	Advanced oxidation processes
Mw	Molecular weight
COD	Chemical oxygen demand
NBB	Naphthol Blue Black
RSM	Response surface methodology
CCD	Composite centered design

Acknowledgement

The authors acknowledge the financial support of this work by University Badji-Mokhtar of Annaba, Algeria.

References

Abdel-Fattah Y.R., Soliman N.A., Gaballa A.A., Sabry S.A., Ei-Diwany A.I.N., Lipase production from a novel thermophilic Bacillus sp: application of Plackett-Burman design for evaluating culture

conditions affecting enzyme formation, Acta Microbiology 51 (2002) 353–366.

Alalm M.G., Tawfik A., Ookawara S., Degradation of four pharmaceuticals by solar photo- Fenton process: Kinetics and costs estimation, Journal of Environment Chemical Engineering 3 (2014) 46–51.

Arslan-Alaton I., Tureli G., Olmez-Hanci T., Treatment of azo dye production wastewaters using photo-Fenton-like advanced oxidation processes: optimization by response surface methodology, Journal of Photochemistry and Photobiology A 202 (2009) 142–153.

Benoist D., Tourbier Y., Germain-Tourbier S., Plans d'expériences: construction et analyse (1995).

Bouafia S., Degradation of textile dyes by advanced oxidation processes based on the fenton reaction, Ph.D Thesis, Saâd Dahlab University Blida, Algeria, (2010).

Bouasla C., Samar M.E.H., Ismail F., Degradation of Methyl Violet 6B by the Fenton process, Desalination 254 (2010) 35-41.

Bouziane L., Bendebane F., Ismail F., Delimi R., Removal of zinc and cadmium from an aqueous solution using sawdust as a low-cost adsorbent: application of Plackett–Burman design, Desalination and Water Treatment 49 (2012) 189-199.

Chergui–Bouafia S., and Alloune R., Procédé d'oxydation avancée pour le traitement des eaux usées: Principe et applications, Revue des Energies Renouvelables ICRESD-07 Tlemcen (2007) 163-170.

Coupez T. et Nouatin A.I, Optimisation of forming by using the simplexe method and preliminary results on an explicit 3D viscoelastic solution, J.A Covas, 2nd Esaform Conference, Guimares (1990) 477-480.

Ertugay N., and Acar F.N., Removal of COD and color from Direct Blue 71 azo dye wastewater by Fenton's oxidation: Kinetic study, Arabian Journal of Chemistry 10 (2017) 1158–1163.

Dulman V., Cucu-Man S.M., Olariu R.I., Buhaceanu R., Dumitras M., Bunia I., A new heterogeneous catalytic system for decolorization and mineralization of Orange G acid dye based on hydrogen peroxide and a macroporous chelating polymer, Dyes and Pigments 95 (2012) 79-88.

Fernandes N.C., Brito L.B., Costa G.G., Taveira S.F., Cunha–Filho M.S.S., Oliveirac G.A.R., Marreto R.N., Removal of azo dye using Fenton and Fenton-like processes: Evaluation of process factors by Box–Behnken design and ecotoxicity tests, Chemico-Biological Interactions 291 (2018) 47-54.

Grigorév A.E., Makarov I.E., Pikaev A.K., Formation of $Cl_2^{\bullet-}$ in the bulk solution during the radiolysis of concentrated aqueous solutions of chlorides, High Energy Chemistry 2 (1987) 99–102.

Gulkaya I., Surucu G.A., Dilek F.B., Importance of H_2O_2/Fe^{2+} ration in fenton's treatement of a carpet dyeing wastewater, Journal of Hazardous Materials 136 (2006) 763-769.

Hammami S., Oturan N., Bellakhel N., Dachraoui M., Otutan M., An oxidative degradation of direct orange 61 by electro-fenton process using a carbon felt electrode, Application of the experimental desing methodology, Journal of Electroanalytical Chemistry 610 (2007) 75-84.

Hayarpi S., Dimitra N., Kyriazis R., Eleni D., Effective biotransfermation of reactive black 5 dye using crude protease from bacillus cereus strain KM201428, Energy Procedia 157 (2019) 815-824.

Iso 3534-3, Statistique–vocabulaire et symboles–partie 3 : plans d'expérience, https://www.iso.org/fr/standard/44245.html (2013).

Kallia E., and Talvenma P., Environmental profile of textile wet processing in Finland, Journal of Cleaner Production 8 (2000) 143-154.

Kavitha V., and Palanivelu K., Destruction of cresols by Fenton oxidation process, Water Research 39 (2005) 3062–3072.

Kochany J., and Lipczynska-Kochany E., Utilization of landfill leachate parameters for pretreatment by Fenton reaction and struvite precipitation—a comparative study, Journal of Hazardous Materials 166 (2009) 248–254.

Kwon B.G., Lee D.S., Kang N., Yoon J., Characteristics of p-chlorophenol oxidation by Fenton's reagent, Water Research 29 (1995) 2206–2210.

Laiju A.R., Sivasankar T., Nidheesh P.V., Iron-loaded mangosteen as a 3 heterogeneous Fenton catalyst for the treatment of landfill leachate, Environmental Science Pollution 21 (2014) 10900–10907.

Lounis M., Samar M.E.H., Hamdaoui O., Sono-electrochemical degradation of Orange G in pure water, natural water, and seawater: effect of operating parameters, Desalination and Water Treatment 57 (2016) 22533-22542.

Nidheesh P.V., Gandhimathi R., Ramesh S.T., Degradation of dyes from aqueous solution by Fenton processes: a review, Environmental Science and Pollution Research 20 (2013) 2099–2132.

Nidheesh P.V., and Rajan R., Removal of rhodamine B from a water medium using hydroxyl and sulphate radicals generated by iron loaded activated carbon, RSC Advances 622 (2016) 330–5340.

Meddah S, Djeghader I., Samar M.E.H., Effect of the operating parameters on the discoloration of the Black Azo Dye Blue Naphthol (NBB) by the Fenton process, Revue Synthèse 26 (2020) 10-24.

Panda N., Sahoo H., Mohapatra S., Decolourization of Methyl Orange using Fenton- 7 like mesoporous Fe_2O_3-SiO_2 composite, Journal of Hazardous Materials 185 (2011) 359-365.

Pignatello J.J., Dark and photoassisted Fe^{3+} catalyzed degradation of chlorophenoxy herbicides by hydrogen peroxide, Environmental Science and Technology 26 (1992) 944-951.

Randrianantoandro T., Rakotobe R., Razafimandimby H., Rakotondrazaka H., Raharimalala L., Rakotonirina T., Etude des répercussions de la pollution industrielle sur la riziculture dans la plaine de Laniera a Antananarivo, Madagascar, Afrique Science 10 (2014) 45-60.

Ribeiro M.C.M., Starling M.C.V.M., Leão M.M.D., Costa de Amorim C., Textile wastewater reuse after additional treatment by Fenton ' s reagent, Environmental Science and Pollution Research 24 (2017) 6165–6175.

Seong J.K., Kwang S.K., Ho J., Optimization of manufacturing parameters for a bracke linling using Taghauchi method, Journal of Materials Processing Technology 136 (2003) 202-208.

Sun J.H., Sun S.P., Wang G.L., Qiao L.P., Degradation of azo dye amido black 10 B in aqueous solution by Fenton oxidation process, Dyes and Pigments 74 (2007) 647-652.

Sun J.H., Sun S.P., Wang G.L., Qiao L.P., Modeling the oxidation kinetics of Fenton's process on the degradation of hemic acid, Journal of Hazardous Materials 179 (2007) 533-539.

Tunçn S., Gurkan T., Duman O., On line spectrophotometric method for the determination of optimum operation parameters on the decolorization of acid red 66 and direct blue 71 from aqueous solution by Fenton process, Chemical Engineering Journal 182 (2012) 431-442.

Verma M., and Haritash A.K., Degradation of amoxicillin by Fenton and Fenton-integrated hybridoxidation processes, Journal of Environmental Chemical Engineering 7 (2019) 1-5.

Xavier S., Gandhimathi R., Nidheesh P.V., Ramesh S.T., Comparison of homogeneous and heterogeneous Fenton processes for the removal of reactive dye 18 magenta MB from aqueous solution, Desalination and Water Treatment 53 (2015) 109–118.

Yingying L., Yan F., Xue L., Ning S., Hao C., Zhongwei W., Removal of diclofenac by three-dimensional electro-Fenton-persulfate (3D electro-Fenton-PS), Chemosphere 219 (2019) 1024-1031.

Zaviska F., Drogui P., Mercier G., Blais J., Procédés d'oxydation avancée dans le traitement des eaux et des effluents industriels: Application à la dégradation des polluants réfractaires, Revue des Sciences de l'Eau 22 (2009) 535–564.

Zhiyu W., Permit trading with flow pollution and stock pollution, Journal of Environmental Economics and Management 91 (2018) 118-132.